Two-dimensional magnetization exchange spectroscopy of Anabaena 7120 ferredoxin. Nuclear Overhauser effect and electron self-exchange cross peaks from amino acid residues surroundi...

ARTICLE *in* BIOCHEMISTRY · JULY 1991

Impact Factor: 3.02 · Source: PubMed

Two-Dimensional Magnetization Exchange Spectroscopy of *Anabaena* 7120 Ferredoxin. Nuclear Overhauser Effect and Electron Self-Exchange Cross Peaks from Amino Acid Residues Surrounding the 2Fe–2S* Cluster[†,‡]

Lars Skjeldal,[§,∥] William M. Westler,[§] Byung-Ha Oh,[§,⊥] Andrzej M. Krezel,[§] Hazel M. Holden,[▽] Bruce L. Jacobson,[▽] Ivan Rayment,[▽] and John L. Markley*[,§]

National Magnetic Resonance Facility at Madison, Institute for Enzyme Research, and Biochemistry and Chemistry Departments, University of Wisconsin, Madison, Wisconsin 53706

Received April 22, 1991; Revised Manuscript Received May 31, 1991

ABSTRACT: Hyperfine ^{1}H NMR signals of the 2Fe–2S* vegetative ferredoxin from *Anabaena* 7120 have been studied by two-dimensional (2D) magnetization exchange spectroscopy. The rapid longitudinal relaxation rates of these signals required the use of very short nuclear Overhauser effect (NOE) mixing times (0.5–20 ms). The resulting pattern of NOE cross-relaxation peaks when combined with previous 1D NOE results [Dugad, L. B., La Mar, G. N., Banci, L., & Bertini, I. (1990) *Biochemistry 29*, 2263–2271] led to elucidation of the carbon-bound proton spin systems from each of the four cysteines ligated to the 2Fe–2S* cluster in the reduced ferredoxin. Additional NOE cross peaks were observed that provide information about other amino acid residues that interact with the iron–sulfur cluster. NOE cross peaks were assigned tentatively to Leu^{27}, Arg^{42}, and Ala^{43} on the basis of the X-ray coordinates of oxidized *Anabaena* 7120 ferredoxin [Rypniewski, W. R., Breiter, D. R., Benning, M. M., Wesenberg, G., Oh, B.-H., Markley, J. L., Rayment, I., & Holden, H. M. (1991) *Biochemistry 30*, 4126–4131]. Three chemical exchange cross peaks were detected in magnetization exchange spectra of half-reduced ferredoxin and assigned to the $^1H^{\alpha}$ protons of Cys^{49} and Cys^{79} [both of whose sulfur atoms are ligated to Fe(III)] and Arg^{42} (whose amide nitrogen is hydrogen-bonded to one of the inorganic sulfurs of the 2Fe–2S* cluster). The chemical exchange cross peaks provide a means of extending assignments in the spectrum of reduced ferredoxin to assignments in the spectrum of the oxidized protein. Our results suggest that 2D magnetization exchange spectroscopy employing short mixing times will be useful for the assignment and characterization of hyperfine ^{1}H peaks in a variety of paramagnetic proteins.

In macromolecules, magnetization exchange by chemical exchange and cross relaxation (the nuclear Overhauser effect or NOE)[1] are formally equivalent (Noggle & Schirmer, 1971; Neuhaus & Williamson, 1989). The first magnetization exchange investigation of a paramagnetic protein was the classic pulsed NMR study of chemical self-exchange in a mixture of oxidized and reduced cytochrome *c* (Redfield & Gupta, 1971). Cross-relaxation (NOE) studies of paramagnetically shifted (hyperfine) resonances appeared later (Gordon & Wüthrich, 1978) and became a valuable tool for spectral assignments, particularly in heme proteins (Trewhella et al., 1979; Keller & Wüthrich, 1980; Lecomte et al., 1985).

Hyperfine proton signals of iron–sulfur proteins were first reported by Poe et al. (1970). The hyperfine signals of ferredoxins generally are characterized by their relative intensities (number of protons) and by the magnitudes and temperature dependencies of their chemical shifts [reviewed by Markley et al. (1986)]. Two new strategies have been used recently to assign ferredoxin hyperfine proton resonances: incorporation of deuterium-labeled cysteine into the protein (Cheng et al., 1990) and detection of one-dimensional (1D) nuclear Overhauser enhancements (NOE's) (Dugad et al., 1990). The latter approach led to preliminary sequence-specific assignments of several of the cysteine proton resonances in the ferredoxins from *Spirulina platensis* and *Prophyra umbilicalis* (Dugad et al., 1990).

Weak NOE's present in regions of overlapping peaks are difficult to detect in 1D difference spectra; they should be more easily resolved in 2D NOE spectra. We show here that hyperfine 2D magnetization exchange spectroscopy can be carried out with a ferredoxin provided that short mixing times and rapid recycle times are used in the data collection. Analysis of the patterns of NOE cross peaks from reduced *Anabaena* 7120 ferredoxin enabled us to characterize the proton spin systems of all four cysteine ligands to the 2Fe–2S* cluster plus those of three other residues located near the cluster. In addition, chemical exchange cross peaks found in 2D magnetization exchange spectra of half-reduced ferredoxin

[†] This work was supported by USDA Grant 88-37262-3406 (J.L.M.) and NIH Grant GM39082 (H.M.H.). NMR studies were carried out in the National Magnetic Resonance Facility at Madison, which is supported by NIH Grant RR02301. Equipment in the NMR Facility was purchased with funds from the NIH Biomedical Research Technology Program (Grant RR02301), the University of Wisconsin, the NSF Biological Instrumentation Program (Grant DMB-8415048), NIH Shared Instrumentation Program (Grant RR02781), and the U.S. Department of Agriculture. L.S. was supported by a grant from the Norwegian Research Council for Science and the Humanities (NAVF).

[‡] NMR data will be deposited in BioMagResBank (Ulrich et al., 1989) under ref ID 889.

[§] National Magnetic Resonance Facility at Madison and Biochemistry Department.

[∥] Present address: University of Trondheim, Kjemisk Institute, Rosenborg, 7055 Dragvoll, Norway.

[⊥] Present address: Department of Chemistry, University of California, Berkeley, CA 94720.

[▽] Institute for Enzyme Research and Chemistry Department.

[1] Abbreviations: Fd, ferredoxin; FID, free induction decay; NOE, nuclear Overhauser effect; NOESY, nuclear Overhauser effect spectroscopy; pH*, pH meter reading (glass electroue calibrated with normal buffers) of a sample dissolved in ^2H_2O uncorrected for deuterium isotope effects; T_1, spin–lattice relaxation time; TPPI, time-proportional phase incrementation, TSP, 3-(trimethylsilyl)propionate.

0006-2960/91/0430-7363$02.50/0

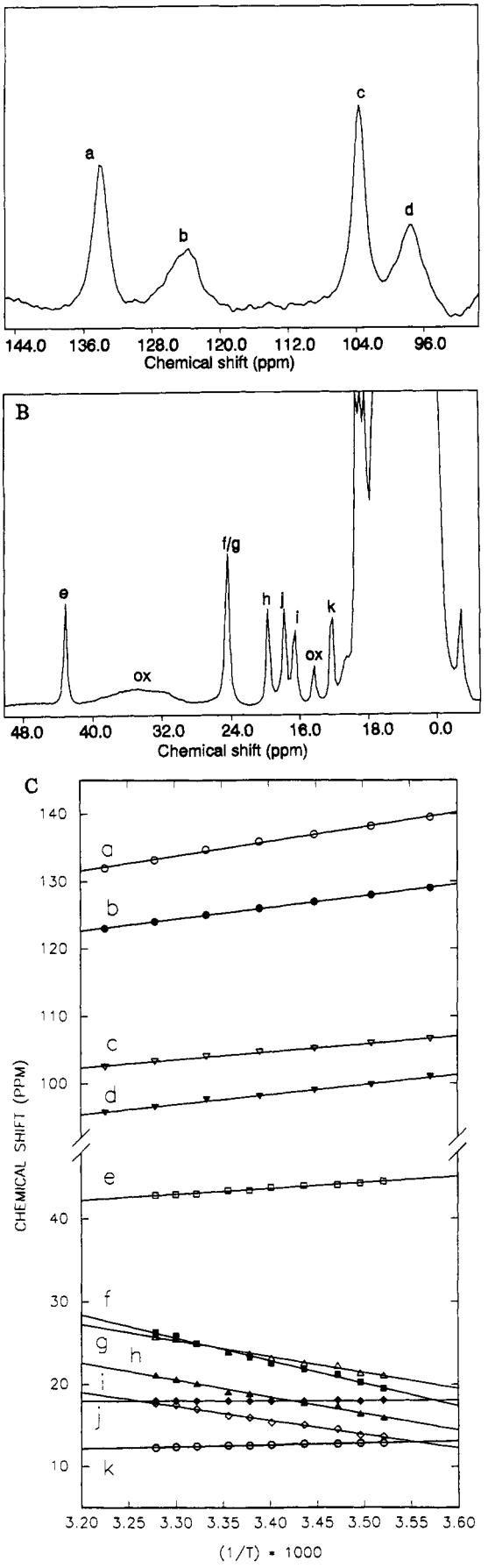

FIGURE 1: Low-field region of the one-dimensional ^1H NMR spectra of (A) oxidized and (B) reduced *Anabaena* 7120 vegetative ferredoxin at 27 °C and pH* 8.2. The labeling convention used for peaks in the reduced ferredoxin is consistent with that of Dugad et al. (1990). (C) Temperature dependence of hyperfine signals (a–k) in reduced *Anabaena* 7120 vegetative ferredoxin.

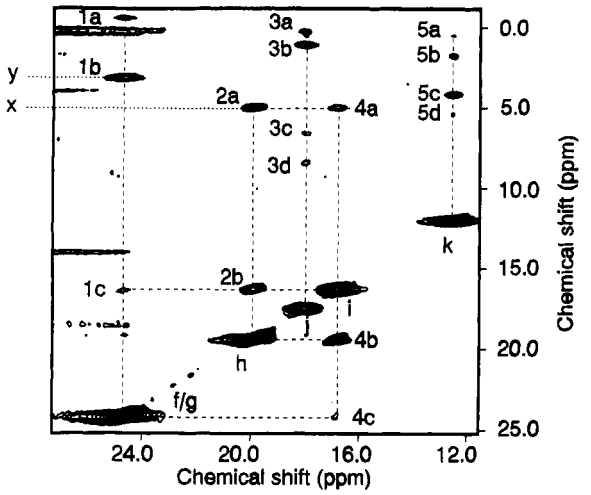

FIGURE 2: Portion of the 600-MHz NOESY spectrum of reduced *Anabaena* 7120 vegetative ferredoxin obtained at 27 °C and pH* 8.2. The intense signals (f–j) are from hyperfine peaks on the diagonal (dashed line). The cross peaks labeled with asterisks (*) arise from cross relaxation between these hyperfine peaks and diamagnetic peaks or other hyperfine peaks. The results are summarized in Table I. Experimental details: 3000 scans/block; 17 ppm carrier frequency; 55.5 ppm spectral width; acquisition time 61 ms; the relaxation delay was set to zero; data size, 4096 × 512 points; 50 dummy scans; 10-ms mixing time.

allowed us to correlate resonances from individual protons in the oxidized and reduced forms of the ferredoxin.

Experimental Procedures

Ferredoxin was isolated from the vegetative form of *Anabaena* 7120 as described previously (Oh & Markley, 1990a). Samples were reduced (totally or half) as described by Skjeldal et al. (1990). Protein samples used for NMR experiments were dissolved in 0.5 mL of a 50 mM phosphate buffer in ^2H_2O. The pH* was 8.2. The final protein concentration was 4 mM. The oxidation state of the protein sample was checked by analysis of 1D ^1H NMR spectra obtained before and after each NOESY data set was collected (Skjeldal et al., 1990).

NMR data were collected on a Bruker AM 600-MHz spectrometer. ^1H NOESY experiments (Macura & Ernst, 1980; Anil Kumar et al., 1980) were collected in the pure absorption mode. The TPPI method (Marion & Wüthrich, 1983) was used for quadrature detection in the second dimension. The receiver and transmitter were aligned to decrease baseline distortions (Marion & Bax, 1988). The NOESY mixing times were between 0.5 and 20 ms, as specified along with other details for individual experiments in the figure captions. ^1H chemical shifts are referenced to internal 3-(trimethylsilyl)propionate (TSP), which was assigned as 0 ppm.

Results and Discussion

One-dimensional ^1H NMR data from reduced *Anabaena* 7120 vegetative ferredoxin are shown in Figure 1. Peaks a–e, j, and k show weak Curie-type temperature dependence (the peaks shift toward their diamagnetic positions as the temperature is raised) whereas peaks f–i show anti-Curie temperature dependence (the peaks shift away from their diamagnetic positions as the temperature is raised) (Chan & Markley, 1983; Skjeldal et al., 1990). Signals with Curie scalar shifts are assigned to protons on residues that are ligated to Fe(III), and signals with anti-Curie scalar shifts are assigned to protons on residues that are ligated to Fe(II) (Dunham et al., 1971; Bertini et al., 1984).

Table I: Hyperfine Related Two-Dimensional NOESY Cross Peaks Observed in the Spectrum of Reduced *Anabaena* 7120 Vegetative Ferredoxin in ^2H_2O Solution, pH* 8.2, and 27 °C

cross peak designation[a]	connectivity[b]		assignments	distance[c] (Å)
	chemical shifts (ppm)	diagonal peaks[d]		
1a	−0.56, 24.72	−, f	$Ala^{43}H_3^{\beta}$, $Cys^{41}H^{\beta 2}$	3.73 (3.56)
1b	3.20, 24.72	−, f/g	$Cys^{41}H^{\alpha}$, $Cys^{41}H^{\beta 3/\beta 2}$	2.55/2.32
1c	16.38, 24.72	i, g	$Cys^{46}H^{\beta 3}$, $Cys^{41}H^{\beta 3}$	2.98
2a	5.00, 19.97	−, h	$Cys^{46}H^{\alpha}$, $Cys^{46}H^{\beta 2}$	2.29
2b	16.33, 19.97	i, h	$Cys^{46}H^{\beta 3}$, $Cys^{46}H^{\beta 2}$	1.76
3a	0.29, 18.04	−, j	$Leu^{27}H_3^{\delta 1}$, $Cys^{79}H^{\alpha}$	5.09 (5.04)
3b	1.08, 18.04	−, j	$Leu^{27}H_3^{\delta 2}$, $Cys^{79}H^{\alpha}$	3.16 (3.07)
3c	6.64, 18.04	−, j	$Leu^{27}H^{\beta 2}$, $Cys^{79}H^{\alpha}$	2.53
3d	8.39, 18.04	−, j	$Leu^{27}H^{\beta 3}$, $Cys^{79}H^{\alpha}$	2.09
4a	5.05, 16.89	−, i	$Cys^{46}H^{\alpha}$, $Cys^{46}H^{\beta 3}$	2.56
4b	19.45, 16.89	h, i	$Cys^{46}H^{\beta 2}$, $Cys^{46}H^{\beta 3}$	1.76
4c	24.16, 16.89	g, i	$Cys^{41}H^{\beta 3}$, $Cys^{46}H^{\beta 3}$	2.98
5a	0.055, 12.57	−, k	$Arg^{42}H^{\beta 2}$, $Arg^{42}H^{\alpha}$	2.96
5b	1.77, 12.57	−, k	$Arg^{42}H^{\beta 3}$, $Arg^{42}H^{\alpha}$	2.64
5c	4.20, 12.57	−, k	$Arg^{42}H^{\gamma 2}$, $Arg^{42}H^{\alpha}$	2.28
5d	5.47, 12.57	−, k	$Arg^{42}H^{\gamma 3}$, $Arg^{42}H^{\alpha}$	2.75

[a] See Figure 2. Peaks f and g overlap at 27 °C. 2D NOE connectivities were observed between these two peaks at 11 °C where they do not overlap (spectrum not shown); they are not listed here. [b] NOE connectivities are given as *i*, *j*, where the dipolar transfer is from *i* to *j*. [c] Hydrogens were added onto the 1.5-Å refinement (manuscript in preparation) of the X-ray structure of oxidized *Anabaena* 7120 vegetative ferridoxin (Rypniewski et al., 1991) by means of the MOLEDT routine of the INSIGHT II graphics molecular modeling package (Biosym Technologies, Inc.). ^1H–^1H distances were measured interactively by using the INSIGHT II software. Average distances were calculated for protons on methyl groups assuming free methyl group rotation. Two distances are given: that outside parentheses is for a third-power average $[(\langle r^{-3}\rangle)^{-1/3}]$, and that within parentheses is for a sixth-power average $[(\langle r^{-6}\rangle)^{-1/6}]$. [d] A dash (−) indicates that the diagonal peak was not observed.

Limited radio frequency pulse power ($\gamma B_1/2\pi \cong 25$ kHz) prevented us from covering the full spectral window in the 2D magnetization exchange experiments. We decided not to include the four peaks at lowest field (a, b, c, and d, Figure 1B). Dugad et al. (1990) did not detect any 1D NOE's among these four peaks, but they found an NOE between peaks a and j and another NOE between peaks c and e. This evidence was used to assign peaks e and j to the $^1H^{\alpha}$ protons of these two cysteines (Dugad et al., 1990). Note that our exchange spectra were obtained at 27 °C, which is below the temperature at which peaks i and j cross (Figure 1D); Dugad et al. (1990) studied *P. umbilicalis* ferredoxin at 30 °C, which is above the temperature at which peaks i and j cross in spectra of that ferredoxin.

NOESY spectra of reduced *Anabaena* 7120 ferredoxin show four cross peaks that correspond to 1D NOE's detected previously in the other plant-type ferredoxins (Dugad et al., 1990): the two cross peaks between f and g (observed in a NOESY spectrum obtained at 11 °C where the peaks do not overlap; spectrum not shown), the two cross peaks between h and i (2b and 4b, Figure 2), and the cross peak between f/g and a methyl (1a, Figure 2). The 2D data (Figure 2) reveal 13 additional NOE connectivities not seen previously: cross peaks 1b and 1c at the frequency of diagonal peaks f/g; cross peak 2a at the frequency of diagonal peak h; cross peaks 3a, 3b, 3c, and 3d at the frequency of diagonal peak j; cross peaks 4a and 4c at the frequency of cross peak i; and cross peaks 5a, 5b, 5c, and 5d at the frequency of cross peak k. The 2D NOE results are summarized in Table I.

Diagonal peaks f and g are assigned to the $^1H^{\beta}$'s of one of the cysteines ligated to Fe(II) (Cys^{41} or Cys^{46}) on the basis of their anti-Curie temperature dependence (Figure 1C). The strong NOE cross peak 1b to diagonal peaks f and/or g (they overlap at 27 °C, Figure 2) can be assigned to the interaction of one or both of the β-protons with the missing $^1H^{\alpha}$ of this cysteine; the corresponding diagonal peak y (not resolved) would be at 3.2 ppm. Dugad et al. (1990) used the 1D NOE between peak f and a methyl peak to distinguish between Cys^{41} and Cys^{46}. According to the X-ray structure of oxidized *S. platensis* ferredoxin (Tsukihara et al., 1981), the closest methyl to a $^1H^{\beta}$ of Cys^{41} is that of Thr^{48} (3.1 Å). The next closest methyl, that of Ala^{43} (5.2 Å), was considered to be too distant to yield an observable NOE.

These residues are conserved in *Anabaena* 7120 vegetative ferredoxin. We reexamined this assignment by adding hydrogens to the refined (1.5-Å) X-ray structure of oxidized *Anabaena* ferredoxin (manuscript in preparation). The results showed that the closest methyl to cysteine-$^1H^{\beta}$ distance is that between the methyl proton of Ala^{43} and the $^1H^{\beta 2}$ of Cys^{41} (2.93 Å). By contrast, the distance between the methyl of Thr^{48} and the closest $^1H^{\beta}$ of Cys^{46} (the $^1H^{\beta 2}$) is 6.62 Å, and that between the methyl of Thr^{48} and the closest $^1H^{\beta}$ of Cys^{41} ($^1H^{\beta 3}$) is 7.41 Å. For this reason, we assign peak f to the $^1H^{\beta 3}$ (*pro-R*) of Cys^{41} and peak g to the $^1H^{\beta 2}$ (*pro-S*) of Cys^{41}.[2]

Cross peaks 1c and 4c (Figure 2) arise from the close proximity of two β-protons, one from each of the two cysteines ligated to Fe(II). The only short distance of this kind found in the *Anabaena* 7120 ferredoxin X-ray structure with added hydrogens is that between the $^1H^{\beta 3}$ (*pro-R*) of Cys^{41} and the $^1H^{\beta 3}$ (*pro-R*) of Cys^{46} (2.98 Å). Thus diagonal peak i is assigned to the $^1H^{\beta 3}$ (*pro-R*) of Cys^{46} and peak h is assigned to the $^1H^{\beta 2}$ (*pro-S*) of Cys^{46}. Cross peaks 2a and 4a link an unobserved diagonal peak x (at 5.0 ppm) with peaks h and i; therefore, x must correspond to the missing $^1H^{\alpha}$ of Cys^{46}.

Peak j, which was assigned to the $^1H^{\alpha}$ of Cys^{79} (Dugad et al., 1990), shows a series of four NOE cross peaks in the methyl (3a, 3b) and methylene (3c, 3d) regions. The only residue in the neighborhood of Cys^{79} (or Cys^{49}) that has this kind of spin system is Leu^{27}. Examination of the *Anabaena* ferredoxin X-ray structure with hydrogens added shows that the two methylene protons of Leu^{27} are close to the Cys^{79} H^{α}; we assign the larger cross peak (3d) to the proton (Leu^{27} $H^{\beta 3}$) at the shorter distance (2.25 Å) and the smaller cross peak (3c) to the proton (Leu^{27} $H^{\beta 2}$) at the longer distance (2.53 Å). The protons of the Leu^{27} $\delta 2$-methyl (*pro-S*) are close to the Cys^{79} H^{α} (closest approach, 2.25 Å); those of the Leu^{27} $\delta 1$-methyl are farther away (4.58 Å). We tentatively assign the stronger NOE cross peak (3b) to the shorter distance and the

[2] The stereochemical designation used here is the *RS* system of Cahn et al. (1966), which has been endorsed by the IUPAC–IUB Joint Commission on Biochemical Nomenclature (1984).

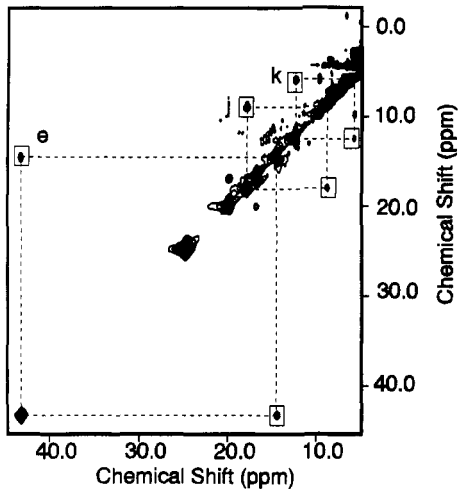

FIGURE 3: Two-dimensional 600-MHz exchange spectrum (NOESY) of half-reduced *Anabaena* 7120 vegetative ferredoxin at 27 °C and pH* 8.2. The dashed line shows the position of the diagonal. The boxed cross peaks, which do not appear in NOESY data from fully reduced ferredoxin (see Figure 2), arise from electronic self-exchange. These cross peaks link the diagonal peaks from protons in the oxidized and reduced states of the ferredoxin. Experimental details: 5600 scans/block; 4.7 ppm carrier frequency; 119 ppm spectral width; acquisition time 29 ms; relaxation delay + acquisition time = 30 ms; data size, 4096 × 512 points; 20 dummy scans; 5-ms mixing time.

weaker NOE cross peak (3a) to the longer distance. No NOE was observed from the $^1H^\alpha$ of Leu^{27}, which is 4.66 Å distant from the Cys^{79} H^α.

All the assigned NOE's correspond to distances less than 3.0 Å with the exception of peak 3a at 4.58 Å assigned to interaction between the Cys^{79} H^α and the Leu^{27} $H^{\delta 1}$. We reexamined the electron density to see if there was any evidence for partial occupancy that might support the existence of rotation about the C^β–C^γ bond but found none. This inconsistency requires further study. If the assignment is correct, the results would indicate either a difference in the structure of the protein in solution and in the crystal or a difference in the structures of the oxidized and reduced proteins.

The combined 1D and 2D NOE data provide the first complete observation of the carbon-bound cysteine proton resonances of a 2Fe–2S* ferredoxin (the cysteine $^1H^N$'s are excluded because the data were collected in ^2H_2O). The only ambiguity remaining in the assignments is whether peak b corresponds to cysteine C (Cys^{49}) and peak d to cysteine D (Cys^{79}) or vice versa (Dugad et al., 1990). Since all the cysteine protons are included in the above assignments, peak k (12.57 ppm, Figure 2), which shows a Curie-type contact shift, must correspond to some other residue, most probably one that is hydrogen-bonded to the iron–sulfur cluster. The four NOE cross peaks (5a–d) arise most likely from nearby protons on the same residue. Of the residues that show potential H-bonds to the iron–sulfur cluster in the X-ray structure of *Anabaena* 7120 ferredoxins (Ser^{40}, Arg^{42}, Ala^{43}, Gly^{44}, Ala^{45}, Thr^{48}, Ser^{47}, Thr^{78}, Val^{80}), all but Arg^{42} and Val^{80} can be ruled out as candidates because their spin systems contain too few protons. Since both Arg^{42} and Val^{80} are potentially hydrogen-bonded to the iron–sulfur cluster by their backbone amide group, we must consider the possibility that the amide proton is protected and may not have exchanged with deuterium in the solvent. Thus we need to consider three possibilities for the assignment of peak k: the $^1H^N$ of Arg^{42}, the $^1H^\alpha$ of Arg^{42}, or the $^1H^N$ of Val^{80}. Upon examining the distances in the *Anabaena* 7120 X-ray structure, the best fit is provided by assigning peak k to the $^1H^\alpha$ of Arg^{42}. With this assignment, all four observed NOE's correspond to distances less than 3.0 Å (Table I); with either of the other two assignment possibilities, one or more of the observed NOE's would have to correspond to a distance in the X-ray structure of over 4.0 Å.

Table II: ^1H NMR Spin Systems of the Cysteines That Ligate the Iron–Sulfur Cluster in Plant-Type 2Fe–2S* Ferredoxins[a]

cysteine	tentative assignment[b]	oxidation state of the ligated iron	peak designation[c] $^1H^{\beta'}$	$^1H^\beta$	$^1H^\alpha$
A	46	Fe(II)	f	g	y
B	41	Fe(II)	h	i	x
C	49	Fe(III)	c	b or d	e
D	79	Fe(III)	a	d or b	j

[a] As deduced from the 1D NOE connectivities of Dugad et al. (1990) and the 2D NOE results reported here. [b] Assignments of cysteine C and D are from Dugad et al. (1990). Dugad et al. assigned peaks h and i to Cys^{41} and peaks f and g to Cys^{46}; the present results reverse these assignments and extend the assignments to the $^1H^\alpha$ resonances, x and y. [c] Peak designations are defined in Figures 1 and 2. By convention (Dugad et al., 1990), $^1H^{\beta'}$ denotes the cysteine geminal proton with the slower relaxation rate and $^1H^\beta$ denotes the geminal proton with the faster relaxation rate. Chiral assignments (Table I) of the β-protons of Cys^{41} and Cys^{46} have been determined here by comparing the NOE data on the reduced ferredoxin with the X-ray structure of the oxidized ferredoxin (Rypniewski et al., 1991).

Table III: Results from the Two-Dimensional Exchange Spectrum (Figure 3) of Half-Reduced *Anabaena* 7120 Vegetative Ferredoxin That Permit the Cross Assignment of Peaks in ^1H Spectra of the Oxidized and Reduced Forms of the Protein

assignment[a]	peak designation, reduced form	chemical shift reduced form	chemical shift oxidized form
cysteine-49 $^1H^\alpha$	e	43.19	14.62
cysteine-79 $^1H^\alpha$	j	17.93	8.88
arginine-42 $^1H^\alpha$	k	12.39	5.81

[a] Assignments of peaks e and j are from Dugad et al. (1990). Peak k is assigned here to Arg^{42} (see Table II and the text).

Electron self-exchange is slow on the NMR time scale when plant-type ferredoxins are reduced with dithionite but fast on the NMR time scale when methyl viologen is added (Skjeldal et al., 1990). The 1D spectrum of *Anabaena* 7120 ferredoxin half-reduced with dithionite appears as the superposition of spectra of the oxidized and reduced forms (Skjeldal et al., 1990). The 2D exchange spectrum obtained with a mixing time of 5 ms (Figure 3) shows six additional cross peaks (enclosed by boxes) that are not present in similar spectra of fully reduced or oxidized protein (Figure 2). These peaks arise from chemical exchange and correlate with chemical shifts of protons in the two redox states. One cross peak links peak e (43.3 ppm) to a resonance at 14.8 ppm. A second cross peak links peak j (18.0 ppm) to a resonance at 9.0 ppm. Peaks e and j are assigned to $^1H^\alpha$ atoms in the two cysteines that ligate Fe(III) in reduced ferredoxin. The 2D exchange results show that the signals from the $^1H^\alpha$ atoms of the cysteines ligated to Fe(III) shift upfield when the other iron is oxidized (Table III).

Conclusion

Hyperfine NMR peaks, which arise from what usually are the most interesting parts of the paramagnetic protein, have been difficult to assign, largely because it appeared that they could not be studied by conventional 2D NMR methods (Oh & Markley, 1990b). The present results indicate that two-dimensional magnetization exchange spectroscopy can be adapted to hyperfine resonances in proteins by the use of short

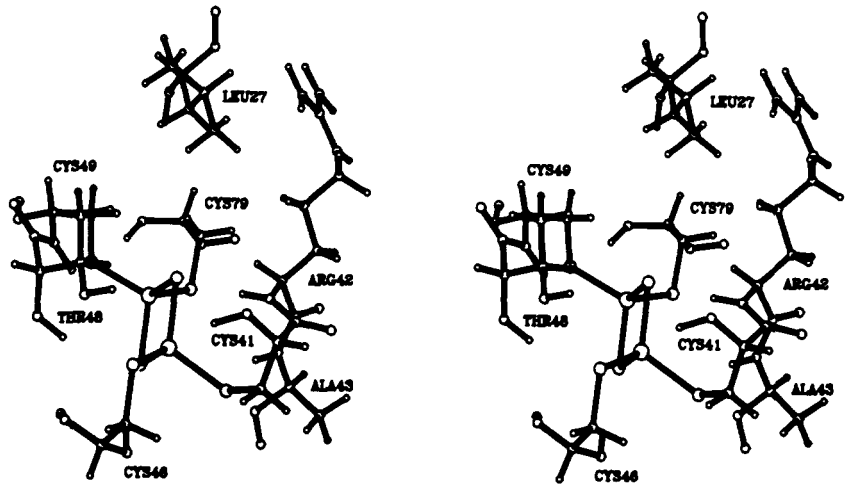

FIGURE 4: Stereoscopic view of the iron–sulfur cluster and selected surrounding residues of oxidized *Anabaena* 7120 vegetative ferredoxin. From the 1.5-Å refinement (manuscript in preparation) of the X-ray structure of this ferredoxin (Rypniewski et al., 1991). Fe1 is the iron ligated to Cys^{41} and Cys^{46}; Fe2 is the iron ligated to Cys^{49} and Cys^{79}.

mixing times and recycle times. The choice of the mixing time depends on the relaxation rates of the protons undergoing magnetization exchange; a theoretical analysis is provided by Cheng (1991). Interproton distances of about 3 Å or less can be sampled by this approach (Table I). Spin diffusion effects should be negligible at the mixing times used. We expect that the optimized NOESY methods used here will be applicable to hyperfine resonances of other paramagnetic proteins. The hyperfine signals of heme proteins have longer relaxation times and can be studied with longer NOESY mixing times (Wu et al., 1991).

The 2D experiments complement and extend 1D NOE results obtained previously on two other plant-type ferredoxins (Dugad et al., 1990). One limitation of the 2D approach stems from the wide chemical shift range that needs to be covered. In the present studies, the best results were obtained when the spectral window was limited to about 36 kHz in each dimension (60 ppm at 600 MHz). We relied on the 1D results for information about the spectral region not covered. For investigations of the more crowded regions, 2D exchange spectroscopy has important advantages over 1D spectroscopy. Only one of the connectivities between the hyperfine and diamagnetic spectral regions found by 2D NOESY (Table I) had been observed in the 1D NMR study: the short distance between a Cys $^1H^{\beta}$ (peak f) and a methyl peak (peak m) (Dugad et al., 1990).

There is a strong theoretical basis (Dunham et al., 1971; Banci et al., 1990) for the division of hyperfine resonances from reduced plant-type ferredoxins into two classes on the basis of their temperature dependence: Curie-type signals from groups that interact with Fe(III) and anti-Curie-type signals from groups that interact with Fe(II). The more detailed assignments of reduced *Anabaena* 7120 vegetative ferredoxin (Tables II and III) were derived here from comparison of the NMR data with the X-ray structure (Figure 4) of oxidized *Anabaena* ferredoxin (Rypniewski et al., 1991). The observed pattern of NOE's shows that the iron ligated to Cys^{41} and Cys^{46} (Fe1 of the X-ray structure) is predominantly Fe(II) and that the iron ligated to Cys^{49} and Cys^{79} (Fe2) is predominantly Fe(III). This result is consistent with interpretations of the X-ray data on oxidized ferredoxins, which show Fe1 to be more exposed and involved in more potential hydrogen-bonding interactions than Fe2 (Tsukihara et al., 1981; Rypniewski et al., 1991).

The NMR assignment method used here relies heavily on the ferredoxin X-ray structure. Since the NMR assignments are of reduced ferredoxin in solution and the X-ray structure is of oxidized ferredoxin in a crystal, implicit assumptions are that the residues near the iron–sulfur cluster do not change their positions significantly on reduction of the protein and that the solution and crystal structures are very similar. Since the diamagnetic resonances of *Anabaena* 7120 ferredoxin do not undergo large chemical shift changes when the redox state is changed (unpublished results from this laboratory), the protein appears not to undergo a large conformational change upon reduction. The earlier assignments (Dugad et al., 1990) were made by reference to an unrefined structure of a closely related ferredoxin. They reported an NOE peak similar to 1a (Figure 2). If they had used the more highly refined X-ray structure used here (Rypniewski et al., 1991), they would have obtained the same assignments of the Cys^{41} and Cys^{46} spin systems reported here rather than the reverse.

Our future aims are to assign the NMR signals by methods that are independent of a crystal structure and to compare the structures of the ferredoxin in the oxidized states by X-ray and NMR methods. It should be possible to test the NMR assignments by selective isotopic labeling; in preparation for such studies, we are optimizing the overexpression of the *Anabaena* 7120 vegetative ferredoxin gene (Alam et al., 1986) in *Escherichia coli*.

The present results demonstrate that the non-cysteine proton that gives rise to peak k in reduced ferredoxin experiences appreciable unpaired spin density. The weak Curie temperature dependence of peak k resonance (Figure 1C) suggests that it is influenced slightly more by the spin on Fe(III) than that on Fe(II). Peak k has been assigned tentatively to the $^1H^{\alpha}$ of Arg^{42} on the basis of comparisons of NOE cross peaks in the spectrum of reduced ferredoxin with the crystal structure of oxidized ferredoxin. The mechanism of electron delocalization presumably is a hydrogen bond between the Arg^{42} $^1H^N$ and the cluster. The X-ray structure of the oxidized ferredoxin shows the Arg^{42} N within hydrogen-bonding distance (3.14 Å) to one of the inorganic sulfur atoms (S1) (Rypniewski et al., 1991). Assuming that the assignment of peak k to the $^1H^{\alpha}$ of Arg^{42} is correct, then its hyperfine shift in oxidized ferredoxin is 1.4 ppm in oxidized ferredoxin (5.8 ppm observed shift minus 4.4 ppm for the diamagnetic chemical shift of an arginine $^1H^{\alpha}$) and 8.0 ppm in reduced ferredoxin (12.4 ppm observed shift minus 4.4 ppm for the diamagnetic chemical shift of an arginine $^1H^{\alpha}$). The magnitude of the hyperfine shift

of peak k in reduced ferredoxin is intermediate between those of the $^1H^{\alpha}$'s of the cysteines ligated to Fe(II) and Fe(III).

Additional evidence for electron delocalization onto at least one nitrogen comes from observation of hyperfine-shifted ^{15}N signals in spectra of *Anabaena* 7120 ferredoxin uniformly labeled with ^{15}N (Oh & Markley, 1990b). Also, a nitrogen component of the ENDOR signal of *Anabaena* 7120 vegetative ferredoxin has been identified by comparing the spectrum of [U-^{15}N]ferredoxin with that of the protein at natural isotopic abundance (A. L. P. Houseman, B.-H. Oh, M. C. Kennedy, L. Fan, M. M. Werst, R. Gurbiel, H. Beinert, J. L. Markley, and B. M. Hoffman, manuscript in preparation). It will be interesting to probe these effects (and to test the NMR assignment of peak k) by selective incorporation of [^{15}N]arginine into the ferredoxin.

It may be significant that Arg^{42} is conserved in 36 of 38 sequences of low potential (plant-type) ferredoxins (Matsubara & Hase, 1983); the two exceptions are ferredoxins II from two species of *Equiseum* (horsetail) in which residue 42 is glutamine. By contrast, residue 42 is histidine in *Anabaena* 7120 heterocyst ferredoxin (Böhme & Haselkorn, 1988), which participates in electron transfer in the nitrogen-fixation system but not in the photosynthetic electron transport system (Böhme & Schrautemeier, 1987). The homologous residue in all sequenced vertebrate ferredoxins (adrenodoxins) is glutamic acid (Mittal et al., 1988). The electronic properties of the latter two proteins differ from those of the photosynthetic ferredoxin. Site-directed mutagenesis can be used to determine whether residue 42 plays a role in these differences.

ACKNOWLEDGMENTS

We thank Mr. Young-Kee Chae and Mr. Andrew P. Hinck for technical assistance and Dr. Gerd N. LaMar for supplying a preprint of his 1D NMR study (Dugad et al., 1990).

REFERENCES

Alam, J., Whitaker, R. A., Krogmann, D. W., & Curtis, S. E. (1986) *J. Bacteriol. 168*, 1265–1271.

Anil Kumar, Ernst, R. R., & Wüthrich, K. (1980) *Biochem. Biophys. Res. Commun. 95*, 1–6.

Banci, L., Bertini, I., & Luchinat, C. (1990) *Struct. Bonding 72*, 113–136.

Bertini, I., Lanini, G., & Luchinat, C. (1984) *Inorg. Chem. 23*, 2729–2730.

Böhme, H., & Schrautemeier, B. (1987) *Biochim. Biophys. Acta 891*, 1–7.

Böhme, H., & Haselkorn, R. (1988) *Mol. Gen. Genet. 214*, 278–285.

Cahn, Ingold, & Prelog (1966) *Angew. Chem., Int. Ed. Engl. 5*, 385–415.

Chan, T.-M., & Markley, J. L. (1983) *Biochemistry 22*, 6008–6010.

Cheng, H. (1991) Ph.D. Thesis, City University of New York.

Cheng, H., Grohmann, K., & Sweeney, W. (1990) *J. Biol. Chem. 265*, 12388–12392.

Dugad, L. B., La Mar, G. N., Banci, L., & Bertini, I. (1990) *Biochemistry 29*, 2263–2271.

Dunham, W. R., Palmer, G., Sands, R. H., & Bearden, A. J. (1971) *Biochim. Biophys. Acta 253*, 373–384.

Gordon, S., & Wüthrich, K. (1978) *J. Am. Chem. Soc. 100*, 7094–7096.

IUPAC–IUB Joint Commission on Biochemical Nomenclature (1984) *Eur. J. Biochem. 138*, 9–37.

Keller, R. M., & Wüthrich, K. (1980) *Biochim. Biophys. Acta 621*, 204–217.

Lecomte, J. T. J., Johnson, R. D., & La Mar, G. N. (1985) *Biochim. Biophys. Acta 829*, 268–274.

Macura, S., & Ernst, R. R. (1980) *Mol. Phys. 41*, 95–117.

Markley, J. L., Chan, T.-M., Krishnamoorthi, R., & Ulrich, E. L. (1986) in *Frontiers of Iron-Sulfur Protein Research* (Matsubara, H., et al., Eds.) pp 167–181, Japan Scientific Societies Press, Tokyo, and Springer-Verlag, Berlin.

Marion, D., & Wüthrich, K. (1983) *Biochem. Biophys. Res. Commun. 113*, 967–974.

Marion, D., & Bax, A. (1988) *J. Magn. Reson. 79*, 352–356.

Matsubara, H., & Hase, T. (1983) in *Proteins and Nucleic Acids in Plant Systematics* (Jensen, U., & Fairbrothers, D. E., Eds.) pp 168–181, Springer-Verlag, Berlin and Heidelberg.

Mittal, S., Zhu, Y.-Z., & Vickery, L. E. (1988) *Arch. Biochem. Biophys. 264*, 383–391.

Neuhaus, D., & Williamson, M. (1989) *The Nuclear Overhauser Effect in Structural and Conformational Analysis*, VCH Publishers, New York.

Noggle, J. S., & Schirmer, R. E. (1971) *The Nuclear Overhauser Effect. Chemical Applications*, Academic Press, New York.

Oh, B.-H., & Markley, J. L. (1990a) *Biochemistry 29*, 3993–4004.

Oh, B.-H., & Markley, J. L. (1990b) *Biochemistry 29*, 4012–4017.

Poe, M., Phillips, W. D., McDonald, C. C., & Lovenberg, W. (1970) *Proc. Natl. Acad. Sci. U.S.A. 65*, 797–804.

Redfield, A. G., & Gupta, R. K. (1971) *Cold Spring Harbor Symp. Quant. Biol. 36*, 405–411.

Rypniewski, W. R., Breiter, D. R., Benning, M. M., Wesenberg, G., Oh, B.-H., Markley, J. L., Rayment, I., & Holden, H. M. (1991) *Biochemistry 30*, 4126–4131.

Skjeldal, L., Westler, W. M., & Markley, J. L. (1990) *Arch. Biochem. Biophys. 278*, 482–485.

Trewhella, J., Wright, P. E., & Appleby, C. A. (1979) *Nature 280*, 87–88.

Tsukihara, T., Fukuyama, K., Nakamura, M., Katsube, Y., Tanaka, N., Kakudo, M., Wada, K., Hase, T., & Matsubara, H. (1981) *J. Biochem. (Tokyo) 90*, 1763–1773.

Ulrich, E. L., Markley, J. L., & Kyogoku, Y. (1989) *Protein Sequences Data Anal. 2*, 23–37.

Wu, J., LaMar, G. N., Yu, L. P., Lee, K.-B., Walker, F. A., Chiu, M. L., & Sligar, S. G. (1991) *Biochemistry 30*, 2156–2165.